Biochimica et Biophysica Acta 1808 (2011) 424–432

Contents lists available at ScienceDirect

Biochimica et Biophysica Acta

journal homepage: www.elsevier.com/locate/bbamem

# Monitoring membrane binding and insertion of peptides by two-color fluorescent label

V.Y. Postupalenko [a], V.V. Shvadchak [a], G. Duportail [a], V.G. Pivovarenko [b], A.S. Klymchenko [a], Y. Mély [a,*]

[a] Laboratoire de Biophotonique et Pharmacologie, UMR 7213 CNRS, Université de Strasbourg, Faculté de Pharmacie, 74, Route du Rhin, 67401 ILLKIRCH Cedex, France
[b] Department of Chemistry, Kyiv National Taras Shevchenko University, 01033 Kyiv, Ukraine

ARTICLE INFO

*Article history:*
Received 22 July 2010
Received in revised form 16 September 2010
Accepted 20 September 2010
Available online 13 October 2010

*Keywords:*
Fluorescence
3-hydroxyflavone
Lipid membrane
Melittin
Peptide–membrane interaction

ABSTRACT

Herein, we developed an approach for monitoring membrane binding and insertion of peptides using a fluorescent environment-sensitive label of the 3-hydroxyflavone family. For this purpose, we labeled the N-terminus of three synthetic peptides, melittin, magainin 2 and poly-L-lysine capable to interact with lipid membranes. Binding of these peptides to lipid vesicles induced a strong fluorescence increase, which enabled to quantify the peptide–membrane interaction. Moreover, the dual emission of the label in these peptides correlated well with the depth of its insertion measured by the parallax quenching method. Thus, in melittin and magainin 2, which show deep insertion of their N-terminus, the label presented a dual emission corresponding to a low polar environment, while the environment of the poly-L-lysine N-terminus was rather polar, consistent with its location close to the bilayer surface. Using spectral deconvolution to distinguish the non-hydrated label species from the hydrated ones and two photon fluorescence microscopy to determine the probe orientation in giant vesicles, we found that the non-hydrated species were vertically oriented in the bilayer and constituted the best indicators for evaluating the depth of the peptide N-terminus in membranes. Thus, this label constitutes an interesting new tool for monitoring membrane binding and insertion of peptides.



## 1. Introduction

Interactions of membrane proteins, peptide toxins and delivery vectors with lipid bilayers play a fundamental role in their activity. However, the precise insertion of the proteins in the bilayer, which is a key element for characterizing the mechanism of these proteins, is difficult to determine experimentally. Fluorescence and notably, fluorescence resonance energy transfer (FRET) is one of the most well-established technique to monitor protein–membrane interactions, through the proximity between fluorescently labeled lipids and peptide. However, the FRET method can hardly be used for precisely localizing a protein/peptide in the membrane, since the FRET signal depends not only on the precise positioning of the FRET partners, but also on their distribution in the lipid bilayer [1]. To localize peptides in membranes, the parallax fluorescence quenching is commonly used. With this method, the Trp residues of a peptide/protein in the bilayer are localized using spin-labeled [2,3] or brominated lipids [4] bearing a quencher at a precise depth. This approach though being universal and rather precise requires a large quantity of quencher (ca 20 mol%) and is limited mainly to model lipid bilayers. Another method that becomes more and more attractive for studying protein insertion is based on environment-sensitive (polarity-sensitive) fluorescent labels. These labels being covalently attached to a peptide chain can change their emission color as a function of the insertion depth (Fig. 1), since the environment polarity varies steeply from the top of the bilayer (dielectric constant $\varepsilon = 80$) to the middle of the bilayer ($\varepsilon \sim 2$). Trp residues, being environment-sensitive fluorophore, can also provide some information about the protein insertion [5,6], but this approach is limited to proteins containing a single Trp residue. Moreover, the fluorescence characteristics and environment-sensitivity of Trp residues show some limitations. Acrylodan and Badan, two reactive derivatives of the common environment-sensitive dye Prodan [7], are among the most popular labels of proteins and peptides used for studying the interactions with lipid membranes. For instance, Acrylodan was used to map the insertion of equinatoxin II into membranes. When labeled mutants of this protein were added to lipid vesicles, only some of them exhibited blue-shifts of the Acrylodan fluorescence, due to insertion of the corresponding peptide labeling site into the hydrophobic membrane environment. These data allowed identification of two protein domains embedded within the lipid membrane [8]. In another study, Acrylodan was used to monitor the insertion of the N-terminal domain of Annexin 2 into lipid bilayers. This insertion was evidenced by blue shifts in its emission and its fluorescence quenching by doxyl-labeled phospholipids [9]. Finally, the Badan label was successfully used to monitor the insertion and orientation of model transmembrane proteins in lipid

* Corresponding author. Tel.: +33 368 854263; fax: +33 368 854313.
*E-mail address:* yves.mely@unistra.fr (Y. Mély).

0005-2736/$ – see front matter © 2010 Elsevier B.V. All rights reserved.
doi:10.1016/j.bbamem.2010.09.013

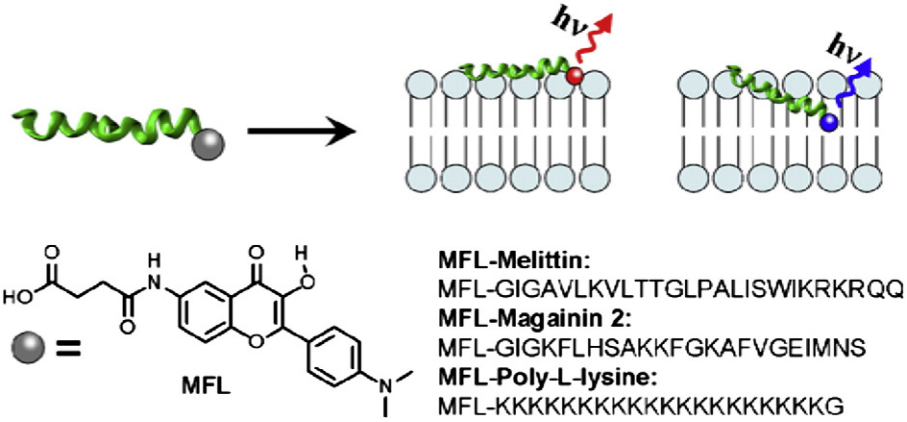


**Fig. 1.** Principle of the monitoring of the interaction of MFL-labeled peptides with the lipid membranes. The peptide (in green) is labeled with the fluorescent MFL label. The interaction of the peptide with lipid membranes changes the fluorescence intensity and color of the label. The extent of these changes depends on the peptide insertion. The chemical structure of the MFL label and its conjugates with peptides are also shown.

membranes, providing complementary information with respect to NMR data and molecular-dynamics simulations [10].

In our studies, we selected a 3-hydroxyflavone fluorophore, 4′-(dimethylamino)-3-hydroxyflavone, which due to excited–state intramolecular proton transfer (ESIPT) and charge transfer presents a strong sensitivity of its dual emission to solvent polarity and hydration [11,12]. This fluorophore has already been used for characterizing the hydration and polarity of model lipid membranes [13–15] and cell plasma membranes [16,17]. In this respect, it was tempting to apply this fluorophore for monitoring interactions of peptides with lipid membranes. As model membrane binding peptides, we selected melittin, magainin 2 and poly-L-lysine. The first two are membranolytic toxins, which bind neutral and charged membranes and insert deeply into the bilayer, producing pores [18–20]. For both melittin and magainin 2, it was reported that their C-terminus is located at the membrane surface, while their N-terminus is inserted rather deeply into the bilayer [21–26]. In contrast, the non viral gene delivery vector, poly-L-lysine [27] binds mainly negatively charged membranes and localizes at the surface next to polar head groups [28]. In the present work, a functionalized fluorescent label, MFL, based on 4′-(dimethylamino)-3-hydraxy-flavone was synthesized and attached to the N-terminus of melittin, magainin 2 and poly-L-lysine (Fig. 1). Studies of the interaction of the labeled peptides with lipid vesicles revealed that peptide–membrane interactions result in a dramatic increase in the fluorescence intensity of the label. All peptides bound to lipid membranes showed a dual emission, which correlated with the depth of the label insertion, as evidenced from parallax quenching measurements. We confirmed that while the N-terminus of melittin and magainin 2 present a rather deep insertion in the bilayer, the poly-L-lysine N-terminus is localized at the interface. Thus, in this work we present a new methodology for monitoring insertion of peptides into lipid bilayers.

## 2. Materials and methods

All chemicals and solvents for synthesis and spectroscopic measurements were from Sigma-Aldrich. Dioleoylphosphatidylcholine (DOPC), dioleoylphosphatidylserine (DOPS) were from Sigma-Aldrich. 1,2-dipalmitoyl-*sn*-glycero-3-phospho(tempo)choline (TempoPC), 1-palmitoyl-2-stearoyl-(5- and 12-doxyl)- *sn*-glycero-3-phosphocholine (5- and 12-SLPC) were from Avanti Polar Lipids (Alabaster, AL, USA). The concentration of phospholipid stock solutions in chloroform was determined by dry weight. The nitroxide content of nitroxide-labeled lipids was calculated using the electron spin resonance integrated spectra of the corresponding diluted stock solutions in chloroform by comparing with a tempocholine reference solution in the same solvent.

### 2.1. Synthesis of MFL label

5′-Acetamido-2′-hydroxyacetophenone (15.5 mmol, 3 g) and 4′-dimethylaminobenzaldehyde (17.1 mmol, 2.55 g) were dissolved in 20 mL of dry DMF. Finally, sodium methoxide (92.6 mmol, 5 g) was added in two portions. The mixture was stirred for 24 h at 60 °C. Then, the reaction mixture was diluted with 100 mL of ethanol followed by addition of 10 mol excess of hydrogen peroxide (16 mL) and 15 mol excess of sodium methoxide (14 g). The reaction mixture was refluxed for 10 min. After cooling, the mixture was poured into water and neutralized with conc. HCl to pH = 6–7. The formed precipitate was filtered off, washed with water, and dried under vacuum. The yellow solid was purified by crystallization from methanol/ethanol mixture to give 6-acetamido-4′-(dimethylamino)-3-hydroxyflavone (2.8 g, 54 %) as yellow crystals. $^1$H NMR (400 MHz, DMSO-d6) $\delta$ 10.22 (s, 1 H), 9.12 (s, 1 H), 8.39 (d, 1 H, J = 2.51 Hz), 8.11 (d, 2 H, J = 9.03 Hz), 7.87 (dd, 1 H, $J_1$ = 9.03 Hz, $J_2$ = 2.51 Hz), 7,68 (d, 1 H, J = 9.03 Hz), 6.85 (d, 2 H, J = 9.03 Hz), 3.02 (s, 6 H) , 2.10 (s, 3 H); *m/z* ($M+H^+$) calculated for $C_{19}H_{19}N_2O_4$: 339.1; found: 339.0.

6-acetamido-4′-(dimethylamino)-3-hydroxyflavone (3 mmol, 1 g) was refluxed in 10% HCl (30 mmol, 11 mL) for 7 h. Then, the reaction mixture was concentrated in vacuo and dissolved in 15 mL dry THF. Then, 0.3 g (3 mmol) of succinic anhydride and 2.6 mL of diisopropylethylamine (15 mmol) were added to this solution. The reaction mixture was stirred overnight at 60 °C. Then the solvent was evaporated and the residue was treated with water. The precipitate was filtered off and washed with water. The product was recrystallized from propanol-2 to give 1 g (yield 84%) of the final acid. $^1$H NMR (300 MHz, DMSO-d6) $\delta$ 12.5–12.0 (1 H, br s), 10.24 (s, 1 H), 9.12 (s, 1 H), 8.40 (d, 1 H, J = 2.64 Hz), 8.09 (d, 2 H, J = 9.04 Hz), 7.84 (dd, 1 H, $J_1$ = 9.04 Hz, $J_2$ = 2.64 Hz), 7,67 (d, 1 H, J = 9.04 Hz), 6.84 (d, 2 H, J = 9.04 Hz), 3.01 (s, 6 H) , 2.65–2.50 (m, 4 H); *m/z* ($M+H^+$) calculated for $C_{21}H_{21}N_2O_6$: 397.1; found: 397.1.

### 2.2. Peptide synthesis

Peptides were synthesized by solid phase peptide synthesis on a 433A synthesizer (ABI, Foster City, CA). The synthesis was performed at a 0.1-mmol scale using standard side-chain protected fluorenylmethoxycarbonyl

(Fmoc)-amino acids and HBTU/HOBt coupling protocol. LL-HMP resin (ABI, 0.44 mmol/g reactive group concentrations) was used as solid support. At the end of the synthesis, peptidylresin was isolated and washed twice by NMP.

Two equivalents (0.15 mmol) of the label (MFL) were dissolved in 1 mL of NMP mixed with two eq. of HBTU/HOBt coupling solution (in DMF) and added to Fmoc-deprotected peptidylresin (0.075 mmol) swelled in 1 mL of NMP. After a few minutes of shaking, five eq. of DIEA solution was added. Then, the reaction mixture was stirred overnight at 40 °C. Resin was filtrated and washed by NMP, methanol and DCM.

Cleavage and deprotection of the peptidylresin were performed for 2 h using a 10 mL trifluoroacetic acid (TFA) solution containing water (5%, v/v), TIS ($iPr_3SiH$, 2.5%, v/v), phenol (1%, w/v), thioanisole (5%, v/v) and ethanedithiol (2.5%, v/v). The solution was concentrated in vacuo and the peptide was precipitated by using ice-cold diethyl ether and then pelleted by centrifugation. The pellet was washed with diethyl ether and dried. The peptides were solubilized with aqueous TFA (0.05 %, v/v). HPLC purification was carried out on a C8 column (uptisphere 300A, 5 μm; 250X10, Interchim, France) in water/acetonitrile mixture containing 0.05% TFA with linear gradients depending on the peptide (typically 10 to 60% of acetonitrile for 30 min) and monitored at 210 nm (detection of all peptides including non-labeled) and 370 nm (detection of labeled peptides only). Molecular masses obtained by ion spray mass spectrometry were: 2844, 3225 and 3017 for MFL-magainin 2, MFL-melittin and MFL-poly-L-lysine, respectively, in agreement with the expected theoretical masses. Prior to use, peptides were dissolved in distilled water, aliquoted and stored at −20 °C. Concentrations of the labeled peptides were determined from the label absorbance at 400 nm using $\varepsilon = 33000\ M^{-1}\ cm^{-1}$.

### 2.3. Sample preparation

Large unilamellar vesicles (LUVs) were obtained by the classical extrusion method [29] or by ethanol dilution [30]. In the first method, a suspension of multilamellar vesicles was extruded by using a Lipex Biomembranes extruder (Vancouver, Canada). The size of the filters was first 0.2 μm (7 passages) and thereafter 0.1 μm (10 passages). This protocol leads to monodisperse LUVs with a mean diameter of 0.11 μm as measured with a Malvern Zetamaster 300 (Malvern, UK).

Giant unilamellar vesicles (GUVs) were generated by electroformation in a home-built liquid cell (University of Odense, Denmark), using previously described procedures [31–33]. 1 mM solution of lipids in chloroform was deposited on the platinum wires of the chamber, and the solvent was evaporated under vacuum for 30 min. The chamber was filled with a 300 mM sucrose solution, and a 2-V, 10-Hz alternating electric current was applied to this capacitor-like configuration for ca. 1.5 h. Then, a 50 μL aliquot of the obtained stock solution of GUVs in sucrose (cooled down to room temperature) was added to 200 μL of 300 mM glucose solution to give the final suspension of GUVs used in microscopy experiments. The staining of GUVs was performed by addition of an aliquot of the peptide solution to obtain a 0.05 μM final concentration.

All measurements were done in 20 mM phosphate buffer containing 150 mM NaCl (pH = 7.4) at 20 °C. To incorporate peptides into the membranes, an aliquot of a peptide stock solution in distilled water was added to a suspension of lipid vesicles. Then the measurements were performed after 5 min of incubation.

### 2.4. Parallax Quenching Method

The fluorescence intensity of labelled vesicles, either DOPC or DOPC with 15% nitroxide lipids, was measured in a 1-cm semi-micro quartz cuvette. Using the corrected $F/F_0$ values, the distance of the fluorophores from the center of the bilayer was calculated using the parallax equation originally proposed by London and collaborators [34–36]:

$$Z_{cf} = L_{cl} + \left[-\ln(F_1 / F_2) / \pi C - L_{21}^2\right] / 2L_{21} \quad (1)$$

where $Z_{cf}$ is the distance of the fluorophore from the center of the bilayer; $F_1$ and $F_2$ are the fluorescence intensities in the presence of the shallow quencher (quencher 1) or the deeper quencher (quencher 2), respectively; $L_{cl}$ is the distance of the shallow quencher from the center of the bilayer, $L_{21}$ is the distance between the shallow and deep quenchers, and $C$ the concentration of quencher in molecules/Å$^2$ (equals the mole fraction of nitroxide-labeled phospholipid divided by area per phospholipid; presently $C = 0.15/70$ Å$^2$ [37]). The quenching by the two most efficient quenchers (TempoPC/5-SLPC or 5-SLPC/12-SLPC) is used to calculate $Z_{cf}$ [34–36]. The values used for the distances of the nitroxide group from the bilayer center were 5.85 Å for 12-SLPC, 12.15 Å for 5-SLPC, and 19.5 Å for TempoPC [34–36].

For quenching experiments by the parallax method, lipid vesicles were prepared according to Kachel et al. [30] with small modifications. DOPC (85%) and nitroxide-labeled PCs (15%) were mixed in chloroform in order to obtain a final concentration of 400 μM. The mixtures were dried under $N_2$ and kept under vacuum for 30 min, and then resuspended in ethanol (120 μL) by continuous rotation using a rotary evaporator for 30 min. Finally, 6 mL of buffer (20 mM phosphate, 150 mM NaCl, pH=7.4) was added and vortexed briefly. The sizes of vesicles were determined by light scattering using a N4SD Coultronics Nanosizer. The vesicles obtained by the ethanol dilution method were of similar size as those obtained by extrusion (0.12 μm). Concentrations of the labeled peptides and lipids were 1 μM (in case of poly-L-lysine −0.05 μM) and 400 μM, respectively.

### 2.5. Deconvolution of spectra

Deconvolution of the fluorescence spectra of the MFL-labeled peptides into three bands, corresponding to the normal (N*), H-bonded normal (H-N*) and tautomer (T*) forms, was performed using the Siano software kindly provided by Dr. A.O. Doroshenko (Kharkov, Ukraine), as previously described [14,15]. The program is based on an iterative nonlinear least-squares method, where the individual emission bands were approximated by a log-normal function accounting for several parameters: maximal amplitude, $I_{max}$, spectral maximum position, $\nu_{max}$, and position of half-maximum amplitudes, $\nu_1$ and $\nu_2$, for the blue and red parts of the band, respectively. These parameters determine the shape parameters of the log-normal function, namely the full width at the half-maximum, $FWHM = \nu_1 - \nu_2$, and the band asymmetry, $P = (\nu_1 - \nu_{max})/(\nu_{max} - \nu_2)$. For the iteration process, the FWHM of the two short-wavelength bands (N* and H–N*) were fixed at 3000 cm$^{-1}$. For the H-N* band, the asymmetry and the band position were fixed at 0.9 and 19000 cm$^{-1}$, respectively. The other parameters, i.e. asymmetry of N* and T* bands, the band width of the T* band and the relative intensities of the bands, were allowed to vary in the iteration process. The resulting fluorescence intensities of the separated N*, H-N* and T* bands ($I_{N^*}$, $I_{H\text{-}N^*}$ and $I_{T^*}$) were used for calculation of the hydration parameter, which was expressed as the ratio of the peak emission intensity of the hydrated (H-N*) form to the summed intensities of the non-hydrated (N* and T*) forms. Taking into account that the FWHM for the T* band is ca 2-fold narrower than for the N* and H-N* bands, the hydration was estimated as $I_{H\text{-}N^*}/(I_{N^*} + 0.5 \times I_{T^*})$. The "polarity" parameter was expressed as the $I_{N^*}/I_{T^*}$ ratio [14,15].

### 2.6. Instrumentation

Proton NMR spectra were recorded on a Bruker spectrometer and mass spectra on a LC/MSD SL Agilent Technologies mass spectrometer using the electrospray ionization (ESI) method. Absorption spectra

were measured on a Cary 4 spectrophotometer (Varian) and fluorescence spectra on a FluoroLog (Jobin Yvon, Horiba) spectrofluorometer. Fluorescence emission spectra were recorded at 400 nm excitation wavelength. All the spectra were corrected for Raman scattering and background fluorescence measured before addition of the labeled peptide. Fluorescence quantum yields were determined by taking 4′-(dialkylamino)-3-hydroxyflavone in ethanol (quantum yield, QY = 0.51) as a reference [12].

To calculate the vesicle concentration, the external radius of the vesicles (R) was considered to be 535 Å, as determined by DLS measurement. The thickness of the lipid bilayer (t) and the average lipid density (d) were assumed to be 40 Å and 70 Å$^2$/lipid, respectively [38]. The number of lipids per vesicle was thus determined as $n = 4\pi^*(R^2 + (R-t)^2)/d = 9.54\times10^4$ lipids /vesicle. The vesicles concentration can thus be obtained by using: $C\ (vesicles) = C\ (lipids)/n$.

To determine the affinity of MFL-melittin for neutral (DOPC) vesicles, a fixed amount of the peptide was titrated with lipids by monitoring the two-band fluorescence of MFL. The fluorescence intensity versus vesicle concentration was plotted and the affinity constant was determined from direct fitting of the curve by the following equation [39]:

$$I = I_0 - \frac{(I_0 - I_t)}{P_t} \times \frac{(1 + (P_t + nN_t)K_a) - \sqrt{(1 + (P_t + nN_t)K_a)^2 - 4P_t nN_t K_a^2}}{2K_a} \quad (2)$$

where $I$ and $I_t$ are the integrated intensity of the whole emission spectrum at a given and a saturating vesicles concentration, respectively, $I_0$ is the corresponding intensity in the absence of vesicles. $N_t$ is the total vesicles concentration, $P_t$ is the total concentration of peptide, $K_a$ is the apparent affinity constant, and n is the number of peptides per vesicle.

Fluorescence microscopy experiments were performed by using a home-built two-photon laser scanning setup based on an Olympus IX70 inverted microscope with an Olympus 60× 1.2NA water immersion objective [40,41]. Two-photon excitation was provided by a titanium-sapphire laser (Tsunami, Spectra Physics), and photons were detected with Avalanche Photodiodes (APD SPCM-AQR-14-FC, Perkin-Elmer) connected to a counter/timer PCI board (PCI6602, National Instrument). Imaging was carried out using two fast galvo-mirrors in the descanned fluorescence collection mode. Typical acquisition time was 5 s with an excitation power around 2.5 mW (830 nm) at the sample. Images corresponding to the blue and red channels were recorded simultaneously using a dichroic mirror (Beamsplitter 585 DCXR) and two APDs. The images were processed with a home-made program under LabView that generates a ratiometric image by dividing the image of the blue channel by that of the red channel. For each pixel, a pseudocolor scale is used for coding the ratio, while the intensity is defined by the integrated intensity recorded for both channels at the corresponding pixel [33].

## 3. Results and discussion

### 3.1. Label design and characterization

The MFL label (Fig. 1) was designed on the basis of 4′-(dimethylamino)-3-hydroxyflavone, a dye displaying high sensitivity to polarity in low polar media [11,42]. It was synthesized in three steps starting from 5-N-acetylamino-2-hydroxyacetophenone. At the final step, the 6-amino-4′-(dimethylamino)-3-hydroxyflavone was reacted with succinic anhydride affording the MFL label. In organic solvents, the MFL label showed absorption and fluorescence properties similar to its parent analogue F. In aprotic media, the probe presented a dual emission, with a short- and a long-wavelength band that could be unambiguously assigned to the normal (N*) and ESIPT tautomer (T*) forms (Fig. 2). While increasing the solvent polarity, the N* band shifted to the red and its relative intensity, $I_{N^*}/I_{T^*}$, increased (Fig. 2, Table 1), in line with our previous studies [11]. In water and other protic media, MFL exhibited a single red-shifted band, corresponding to the emission of the H-bonded N* form (H-N*). In this form, a strong H-bond between the 4-carbonyl group of the flavone and the protic solvent is thought to inhibit the ESIPT reaction [43,44]. Importantly, the fluorescence quantum yield of the label is very low in neat water (Table 1), but not in other protic media like alcohols.

### 3.2. Labeled peptides and peptide–membrane interactions

Using solid-phase peptide synthesis, three peptides labeled by MFL at their N-terminus were obtained: melittin, magainin 2 and poly-L-lysine, which contain 26, 23 and 21 amino acids, respectively (Fig. 1). These peptides present different numbers of basic and hydrophobic amino acids, and bind differently to lipid membranes. In buffer, all three labeled peptides showed a single red-shifted emission band similar to that of the free label, though the fluorescence quantum yield is significantly higher with the peptides. We speculate that the proximal peptide backbone could partially screen the probe from water and, thus reduce its quenching by water.

Addition of DOPC vesicles changed dramatically the fluorescence of the labeled melittin and magainin 2 but not of poly-L-lysine, confirming that only the two first peptides can interact with neutral lipid bilayers. For both melittin and magainin 2, a large increase in the fluorescence quantum yield was accompanied with the appearance of the two-band emission characteristic for the probe in hydrophobic environment (Table 2, Fig. 3). Thus, the interaction of the two peptides with lipid membranes results in the transfer of the label from water into the hydrophobic membrane environment which affects dramatically its emission properties.

The binding stoichiometry is an important characteristic of peptide–lipid interactions. Since the fluorescence of the free peptide differs significantly from that of the membrane-bound peptide, the binding stoichiometry could be determined in a simple titration experiment. For these studies, we selected the interaction between melittin and DOPC vesicles. On addition of the labeled peptide to a suspension of DOPC vesicles, the fluorescence increased linearly with the peptide concentration reaching saturation at a ratio of 1 peptide per 100 lipids. Above this ratio, the intensity remained constant indicating a saturation of the membrane surface by the peptide (Fig. 4A). We performed also a reverse titration by adding increasing

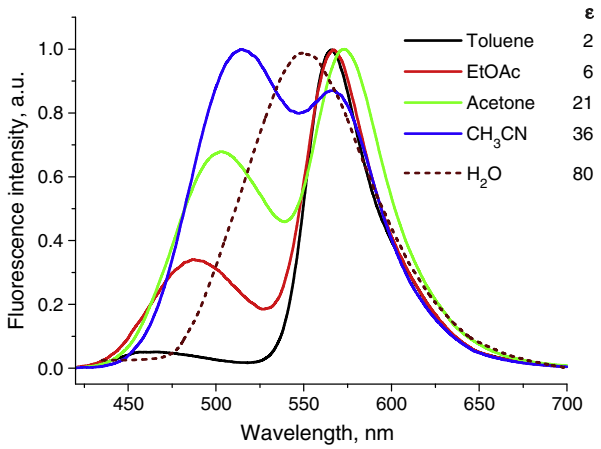


**Fig. 2.** Normalized fluorescence spectra of the MFL label in different solvents. Concentration of MFL was 1 μM. Excitation wavelength was 400 nm.

**Table 1**
Spectroscopic properties of the MFL label in solvents.

| No | Solvent | $\varepsilon$ | $\lambda_{ABS}$, nm | $\lambda_{N^*}$, nm | $\lambda_{T^*}$, nm | $I_{N^*}/I_{T^*}$ | QY |
|---|---|---|---|---|---|---|---|
| 1 | Toluene | 2.37 | 403 | 466 | 566 | 0.05 | 0.226 |
| 2 | EtOAc | 5.99 | 396 | 487 | 567 | 0.34 | 0.095 |
| 3 | Acetone | 20.5 | 398 | 503 | 573 | 0.68 | 0.101 |
| 4 | $CH_3CN$ | 35.7 | 399 | 516[a] | 575[a] | 2.32[a] | 0.154 |
| 5 | EtOH | 24.9 | 408 | 529 | – | – | 0.482 |
| 6 | MeOH | 32.6 | 406 | 533 | – | – | 0.262 |
| 7 | Buffer | 78.4 | 394 | 550 | – | – | 0.004 |

$\varepsilon$—dielectric constant, $\lambda_{ABS}$—position of absorption maxima, $\lambda_{N^*}$ and $\lambda_{T^*}$—position of fluorescence maxima of N* and T* forms, respectively. $I_{N^*}/I_{T^*}$—ratio of the intensities of the two emission bands at their peak maxima (errors are ±2%). QY— fluorescence quantum yield (errors are ±5%), measured using FE in EtOH (QY = 51%) as a reference. 20 mM phosphate buffer, 150 mM NaCl, pH = 7.4 was used. Excitation wavelength was 400 nm.

[a] The values were evaluated from deconvolution of the emission spectra.

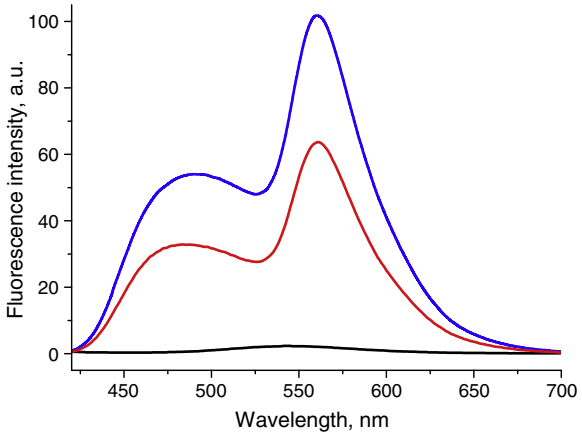


**Fig. 3.** Fluorescence changes on binding of MFL-labeled melittin and magainin 2 to DOPC vesicles. Emission spectra of both peptides in the absence (black) and in the presence of LUVs composed of neutral DOPC lipids (magainin 2—red, melittin—blue). Concentration of peptide and lipids was 0.3 and 100 μM, respectively. Buffer was 20 mM phosphate, 150 mM NaCl, pH = 7.4. Excitation wavelength was 400 nm.

lipid concentrations to a constant concentration of the labeled peptide (Fig. 4B). We observed that the fluorescence intensity reaches saturation at a ratio of 1 peptide per 100 lipids, confirming the lipid/peptide binding stoichiometry. Moreover, this titration curve allowed us to evaluate the binding constant $K = 4 \pm 2 \times 10^7\ M^{-1}$ of melittin to the DOPC membrane.

The ability of the label to monitor the binding of the peptide to the membrane was then used to determine the appropriate lipid composition required for efficient binding of poly-L-lysine to lipid membranes. For this purpose, we studied the fluorescence spectra of the labeled poly-L-lysine in the presence of vesicles containing mixtures of neutral lipid DOPC with different molar fraction of negatively charged lipid DOPS (Fig. 5). A strong (ca 20 times) increase in the fluorescence intensity of the labeled poly-L-lysine was recorded for vesicles, where the content of DOPS exceeded 10 mol% (Fig. 5), which thus represents the critical concentration of negatively charged lipids required for binding of poly-L-lysine. In the further experiments, we used 20 mol% of DOPS in DOPC vesicles, which provides efficient poly-L-lysine binding.

It was also important to monitor by dynamic light scattering the possible aggregation of vesicles in the presence of cationic peptides [45]. Neither melittin, nor magainin 2 affected the size of DOPC/DOPS (80/20 mol%) vesicles at a lipid/probe ratio 400:1, indicating that these peptides do not induce vesicle aggregation in these conditions. In contrast, an aggregation was observed with the highly charged poly-L-lysine (data not shown) at lipid to peptide ratios < 8000/1. Therefore, in further experiments, an 8000:1 ratio was used with poly-L-lysine.

### 3.3. Localizing peptide N-terminus in the membrane

Lipid membranes are complex media, where the polarity and hydration parameters exhibit a steep dependence on the depth in the bilayer [46]. Our label, being sensitive to both of these parameters, can therefore be used for evaluating the insertion depth of the peptide N-terminus to which the probe is covalently bound. Comparison of the dual emission of the peptides bound to lipid vesicles of the same composition (DOPC/DOPS) shows that the relative intensity of the short-wavelength band is much larger for poly-L-lysine than for the two other peptides (Fig. 6A), suggesting that the polarity and/or hydration of the peptide N-terminus is significantly larger for poly-L-lysine. To evaluate quantitatively the hydration and polarity of the label environment in these peptides, we used a methodology well established for membrane probes based on the same fluorophore [14,15]. In this methodology, the apparent two-band emission spectrum is deconvolved into three bands, with the N* and T* bands corresponding to the non-hydrated form of the dye and the H–N* band corresponding to the hydrated form. The H–N* form is usually localized at the hydrated membrane interface and its emission band is strongly red-shifted with respect to the N* band [14,15]. Using this approach, we deconvolved the emission spectra of the peptides bound to DOPC/DOPS vesicles into N*, T* and H–N* bands (Fig. 6B).

**Table 2**
Spectroscopic properties of MFL-labeled peptides.[a]

| Peptide | Media | $\lambda_{ABS}$, nm | $\lambda_{N^*}$, nm | $\lambda_{T^*}$, nm | $I_S/I_L$ | $I_{N^*}/I_{T^*}$ | Hydration | QY |
|---|---|---|---|---|---|---|---|---|
| MFL–Magainin 2 | Buffer | 414 | 547 | – | – | – | – | 0.044 |
| | DOPC | 406 | 475 | 562 | 0.55 | 0.62 | 0.42 | 0.459 |
| | DOPC/DOPS(8/2) | 406 | 474 | 562 | 0.62 | 0.74 | 0.41 | 0.464 |
| MFL–Melittin | Buffer | 408 | 544 | – | – | – | – | 0.022 |
| | DOPC | 406 | 476 | 562 | 0.54 | 0.58 | 0.44 | 0.596 |
| | DOPC/DOPS(8/2) | 406 | 477 | 562 | 0.61 | 0.68 | 0.44 | 0.406 |
| MFL–Poly-L-lysine | Buffer | 410 | 553 | – | – | – | – | 0.032 |
| | DOPC | 414 | 556 | – | – | – | – | 0.048 |
| | DOPC/DOPS(8/2) | ~413 | 474 | 559 | 0.97 | 1.52 | 0.37 | 0.669 |

[a] $\lambda_{ABS}$ is the position of absorption maxima; $\lambda_{N^*}$ and $\lambda_{T^*}$ are the maxima of N* and T* emission bands, respectively; $I_S/I_L$ is the intensity ratio of the short- and long-wavelength bands measured at the peak maxima; $I_{N^*}/I_{T^*}$ is the intensity ratio of the two emission bands measured at the peak maxima obtained from deconvolution of the corresponding spectra into three bands; all data, except quantum yields, refer to LUVs prepared by the ethanol dilution method; quantum yield (QY) measurements were done in LUVs prepared by the extrusion method. Excitation wavelength was 400 nm. Peptide and lipids concentrations were 0.3 and 100 μM, respectively. Buffer is 20 mM phosphate, 150 mM NaCl, pH = 7.4. Estimated errors: $\lambda_{ABS} \pm 2$ nm; $\lambda_{N^*}$, $\lambda_{T^*} \pm 1$ nm; $I_S/I_L \pm 2\%$; $I_{N^*}/I_{T^*} \pm 3\%$; Hydration ± 3%; QY ± 5%.

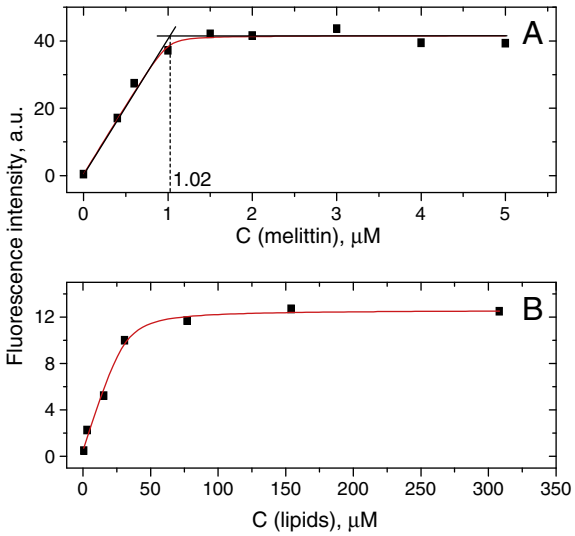


**Fig. 4.** Determination of the binding parameters of MFL-melittin to DOPC vesicles. Titration of 100 μM DOPC vesicles by MFL-melittin (A). Titration of 0.3 μM MFL-melittin by DOPC vesicles (B). The binding constant of MFL-melittin to the DOPC vesicles was determined by fitting (red curve) the data points in B to equation 1 in the materials and methods section.

From the deconvolved spectra, the hydration parameter can be evaluated from the ratio of the peak emission intensity of the hydrated (H–N*) form to the summed intensities of the non-hydrated (N* and T*) forms, while the "polarity" parameter can be evaluated from the $I_{N^*}/I_{T^*}$ ratio. The obtained results show that the hydration parameter is nearly the same for all three peptides, while the polarity parameter is much larger for poly-L-lysine than for the two other peptides (Table 2). Previously, we have established for the same 3HF fluorophore that its $I_{N^*}/I_{T^*}$ ratio in aprotic solvents varies linearly with the dielectric constant function, $f(\varepsilon)=(\varepsilon-1)/(2\varepsilon+1)$ [11] (Fig. 7). Here, we used this linear dependence to estimate the environment polarity of the label (non-hydrated form) in the membrane for the three labeled peptides. We found that for melittin and magainin 2, the observed $I_{N^*}/I_{T^*}$ ratios correspond to a dielectric constant $\varepsilon \sim 10$–11, while for poly-L-lysine, the $I_{N^*}/I_{T^*}$ ratio corresponds to an $\varepsilon$ value close to 39 (Fig. 7). Using the dielectric model of lipid bilayer suggested by Griffith et al [46], these values correspond to depths of ~10 and ~20 Å from the bilayer center, i.e. to the regions of the fatty acid chains and phosphate residues, respectively.

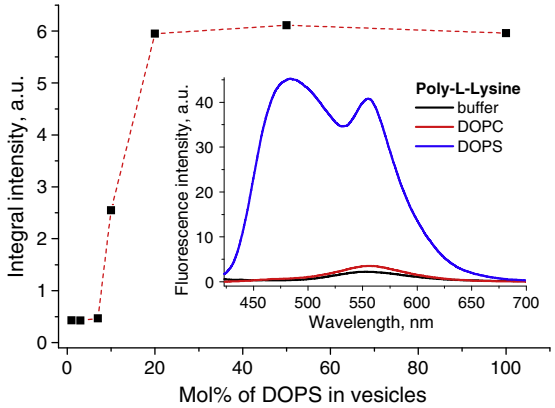


**Fig. 5.** Dependence of poly-L-lysine/LUV binding (integral fluorescence intensity of the label) on the content of negatively charged lipids (DOPS). The dashed red curve is used to connect the data points (squares). Fluorescence spectra of the peptide with and without lipid vesicles are shown in the inset. Concentration of peptide and lipids was 0.3 and 100 μM, respectively. Excitation wavelength was 400 nm.

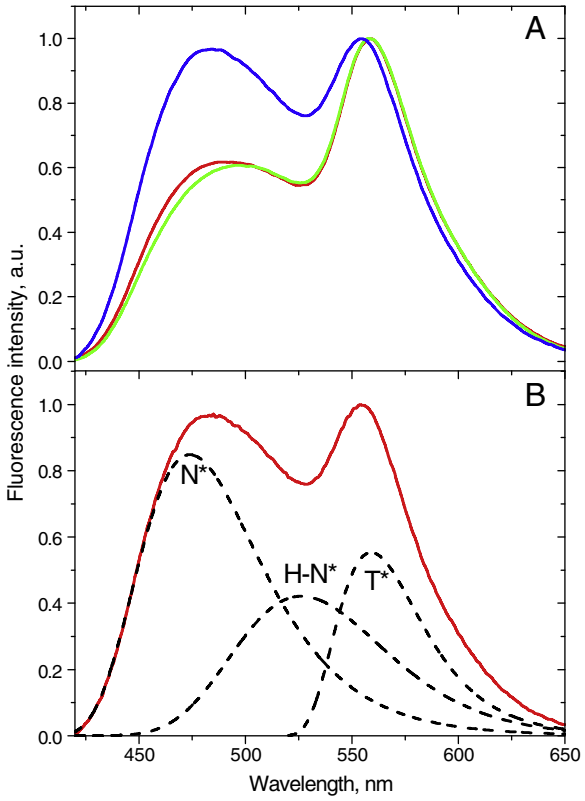


**Fig. 6.** Fluorescence spectra of MFL—melittin, MFL—magainin 2 and MFL—poly-L-lysine bound to DOPC/DOPS (80/20 mol%) vesicles. (A) Normalized fluorescence spectra of MFL—melittin (green), MFL—magainin 2 (red) and MFL—poly-L-lysine (blue) bound to DOPC/DOPS vesicles. (B) Emission spectrum of poly-L-lysine (solid red line) and its deconvolution into N*, H–N*, and T* spectral components. Experiments were performed in 20 mM phosphate buffer, 150 mM NaCl, pH = 7.4, using an excitation wavelength of 400 nm.

An independent measure of the localization of a fluorescent dye in a bilayer can be provided by the parallax quenching method using spin-labeled lipids [34,35]. Previously, using this method we were

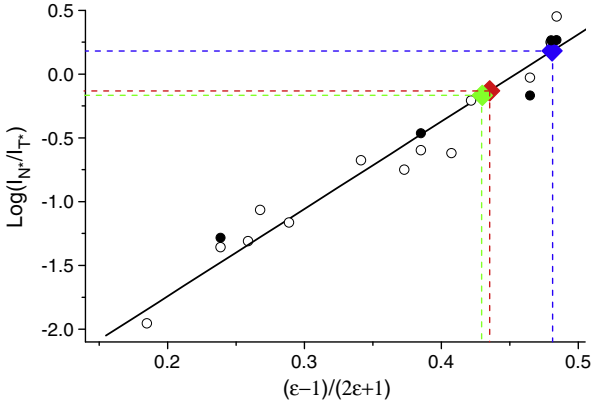


**Fig. 7.** Evaluation of the polarity of the probe environment for the three labeled peptides bound to DOPC/DOPS vesicles. The logarithm of $I_{N^*}/I_{T^*}$ was plotted as a function of the polarity function, $f(\varepsilon)$, for FE (○) (data from ref. [11]) and MFL (●) in different solvents as well as for MFL-magainin 2 (red), MFL-melittin (green) and MFL-poly-L-lysine (blue) bound to DOPC/DOPS (80/20 mol%) vesicles. The data points were fitted (black line) with the following equation: $\log(I_{N^*}/I_{T^*}) = -3.111 + 6.849 f(\varepsilon)$, $r^2 = 0.976$, SD = 0.159.

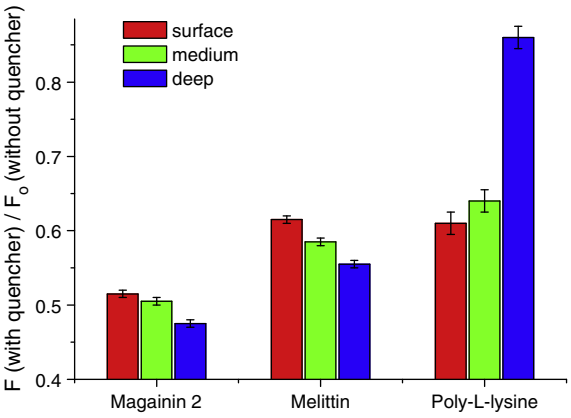


**Fig. 8.** Fluorescence quenching of MFL-magainin 2, MFL-melittin and MFL-poly-L-lysine bound to DOPC/DOPS (80/20 mol%) vesicles containing 15 mol % TempoPC (red), 5-SLPC (green), or 12-SLPC (blue), respectively. The fluorescence intensities of the labeled peptides bound to vesicles in the presence of quenchers were compared to the fluorescence intensities in their absence.

able to localize the fluorophore of membrane probes in lipid membranes [47]. Presently, we used this method to evaluate directly the depth of the labels in the bilayer for all three peptides. Three quenchers of deep (5.85 Å from the bilayer center), middle (12.15 Å) and shallow location (19.5 Å) were used. In a first step, we performed the parallax analysis on the basis of the integral intensity of the whole emission spectrum. For both melittin and magainin 2, the deep quencher was the most efficient, while the shallow quencher was the least efficient (Fig. 8). Using the parallax equation (see Materials and methods), we obtained average depths for melittin and magainin 2 of 8.3–8.4 Å from the bilayer center. In contrast, for poly-L-lysine the quenching was the most efficient with the shallow quencher and the least efficient for the deep quencher (Fig. 8), giving an estimated depth of 16.6 Å. Thus, the parallax analysis of the integral intensity of the whole emission spectra gave us a clear difference in the depths of the label for melittin and magainin 2 in comparison to poly-L-lysine. In a next step, the quenching of the hydrated and non-hydrated forms of the label was analyzed independently after deconvolution of the corresponding emission spectra. The non-hydrated form of the label for melittin and magainin 2 in DOPC/DOPS membrane was found to be located at 8.0–8.1 Å from the bilayer center (Table 3), in the region of the fatty acid chains (Fig. 9), in line with our estimations based on the relatively low dielectric constant of its environment (Fig. 7). The location of the hydrated form of the label for both proteins was 16.4 Å, indicating a shallow position next to the head groups (Fig. 9). Two reasons could explain this large difference in the locations of the two forms of the label. One is the relative freedom of the label, due to the presence of the flexible spacer, which could allow both deep and shallow localizations of the label (Fig. 9). The other reason could be that melittin and magainin 2 present both tilted and surface location in the lipid bilayer, thus producing the observed heterogeneity in depths. Remarkably, for poly-L-lysine, both hydrated and non-hydrated forms present a shallow location close to the head groups, around 16.5 Å from the bilayer center (Table 3, Fig. 9), in line with the high dielectric constant of its environment (Fig. 7). Noticeably, the fluorescence quantum yields were rather close for deeply inserted and shallow peptides, in line with the poor correlation of the fluorescence quantum yield of MFL (Table 1) and its analogues [11] with solvent polarity.

### 3.4. Label orientation

Orientation of the label is a parameter that could also help to understand the behavior of the protein and its label in the bilayer. A direct measurement of the fluorophore orientation in the bilayer of giant vesicles (GUVs) can be performed by fluorescence microscopy using a polarized laser excitation. Fluorophores with a transition dipole moment parallel to the polarization plane are excited preferentially. This method was recently used to determine the orientation of membrane probes based on Prodan [48] and 3HF [33]. In the present work, labeled melittin and poly-L-lysine were added to GUVs composed of DOPC/DOPS and studied by two-photon microscopy. We recorded the images in the blue and red regions, which were then used to calculate the ratio images.

In the case of poly-L-lysine, the intensity recorded for both blue and red channels was highest at the poles of the GUVs, while the lowest intensity was observed on their equator (Fig. 10A and B). This intensity distribution is typical for a fluorophore oriented vertically in the bilayer (orthogonal to the lipid surface, Fig. 9 [33,48]). Moreover, in the ratio image, the color of the poles and equator were almost identical (Fig. 10C), so that the dual emission of the label in this case is independent of the direction of the light polarization. For the labeled melittin, it was found that for the blue channel, the intensity was the same at the poles and equator (Fig. 10D), while for the red channel GUVs are brighter at the poles than at the equator (Fig. 10E). In the ratiometric images, the poles and equator appeared in different colors corresponding to lower and higher $I_{blue}/I_{red}$ ratios, respectively (Fig. 10F). The observed effect of polarization on the emission color suggests two populations for the label in the bilayer. One population is associated with a low $I_{blue}/I_{red}$ ratio (observed mainly in the red channel, Fig. 10E) and orients vertically in the bilayer, while the second population is associated with a high $I_{blue}/I_{red}$ ratio (observed mainly in the blue channel, Fig. 10D) and does not exhibit any preferential orientation. This conclusion corroborates the parallax data, which also suggest two populations for the melittin label: a deep non-hydrated population and a shallow hydrated population. Therefore, we could conclude that the deeply located label population is oriented vertically in the bilayer, while the shallow population presents no preferential orientation. A similar behavior was previously observed for the parent fluorophore F in lipid membranes and to some extent for membrane probes based on the same fluorophore [14,15,33]. In contrast, poly-L-lysine showed no heterogeneity in the probe orientation. Since the N-terminus of this peptide is at the

**Table 3**
Parallax quenching data of non–hydrated and hydrated forms of MFL-labeled magainin 2, melittin and poly-L-lysine in DOPC/DOPS (80/20 mol%) vesicles.[a]

| Peptide | $F_{TC}/F_0$ | $F_5/F_0$ | $F_{12}/F_0$ | $Z_{cf}$, Å | $F_{TC}/F_0$ | $F_5/F_0$ | $F_{12}/F_0$ | $Z_{cf}$, Å | $<Z_{cf}>$, Å |
|---|---|---|---|---|---|---|---|---|---|
| Forms | Non-hydrated form | | | | Hydrated form | | | | Both forms |
| Magainin 2 | 0.53 | 0.52 | 0.48 | 8.0 | 0.43 | 0.45 | 0.44 | 16.4 | 8.3 |
| Melittin | 0.67 | 0.62 | 0.57 | 8.1 | 0.49 | 0.52 | 0.52 | 16.4 | 8.4 |
| Poly-L-lysine | 0.63 | 0.67 | 0.89 | 16.5 | 0.54 | 0.57 | 0.85 | 16.3 | 16.6 |

[a] $F_{TC}/F_0$, $F_5/F_0$, and $F_{12}/F_0$ are the ratios of the fluorescence intensities of the labeled peptides bound to DOPC/DOPS (80/20 mol%) vesicles containing 15 mol % TempoPC, 5-SLPC, or 12-SLPC, respectively, to the corresponding fluorescence intensities in the absence of the nitroxide-labeled lipids. The intensities were obtained by deconvolution of the fluorescence quenching data. The obtained integral intensities of the H–N* form and the sum of the integral intensities of N* and T* forms were used to calculate the quenching for hydrated and non-hydrated forms, respectively. $Z_{cf}$ is the distance between the middle of the bilayer and the chromophore center calculated from the parallax equation. $<Z_{cf}>$ is the average distance calculated from the integral intensity of the label without deconvolution. The estimated error for $Z_{cf}$ is $\pm 1$ Å.

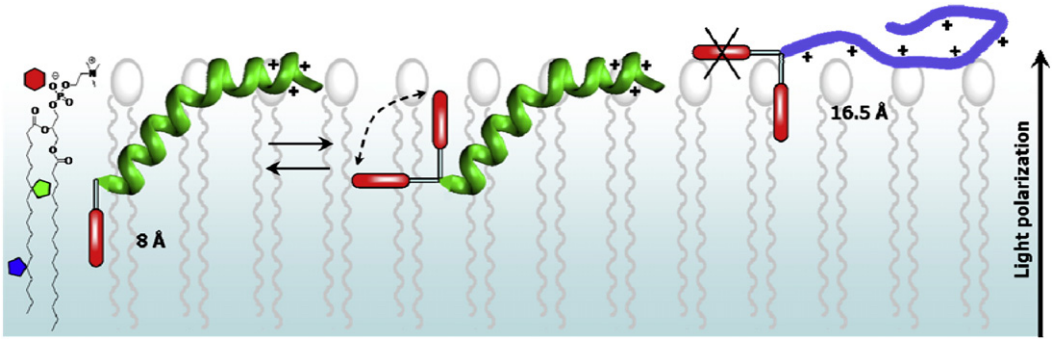


**Fig. 9.** Localization of the N-terminus of melittin (green) and poly-L-lysine (blue) labeled by MFL probe and bound to DOPC/DOPS (80/20 mol%) membrane. The positions of the quenching residues of the deep (blue), middle (green) and shallow (red) quenchers are pointed by the colored polygons. In the case of melittin, two locations of the label are shown: deep vertical (non-hydrated) and shallow with a distribution of orientations (hydrated).

bilayer surface [45], the relatively hydrophobic label likely orients vertically towards the hydrophobic interior of the bilayer (Fig. 9).

The present data illustrate the use of the present label for monitoring membrane binding and insertion of peptides. With this label, the binding of the label peptides to membranes can be readily detected by the strong increase in their fluorescence intensity and appearance of dual emission. Moreover, this label can provide a rapid evaluation of the approximate location of the peptide N-terminus by simply recording the ratio of its two emission bands. Importantly, the N-terminus localization of both deeply inserted (melittin and magainin 2) and surface located (poly-L-lysine) peptides, estimated by our approach, is in agreement with the literature data [21–26,28,45], suggesting that the MFL label did not change significantly the peptide insertion. However, the precision of this location is limited by the flexibility of the linker group, which allows delocalization of the probe, with different depths and orientations. This problem of label delocalization is partly avoided by distinguishing non-hydrated and hydrated species. Indeed, we observed that the non-hydrated species of the dye presents mainly a vertical orientation, and its depth correlates well with the protein insertion. In contrast, hydrated species are located at the surface, independently of the peptide insertion, allowing multiple orientations of the probe (Fig. 9). Thus, it is important to remove the hydrated species from the analysis, which can successfully be realized by spectral deconvolution. As a consequence, the $N^*/T^*$ ratio, describing the polarity of non-hydrated species appears as a good indicator of protein insertion. In the future, further improvement in the location of the probe will be achieved by attaching it rigidly to the peptide backbone, as it has already been done with fluorine- and spin-labels for NMR [49,50] and EPR [51] spectroscopy, respectively. Moreover, the precision of the depth estimation based on the measured dielectric constant will also benefit from a better definition of the exact profile of the dielectric constant across the lipid membrane, which is still a matter of discussion [46,52,53].

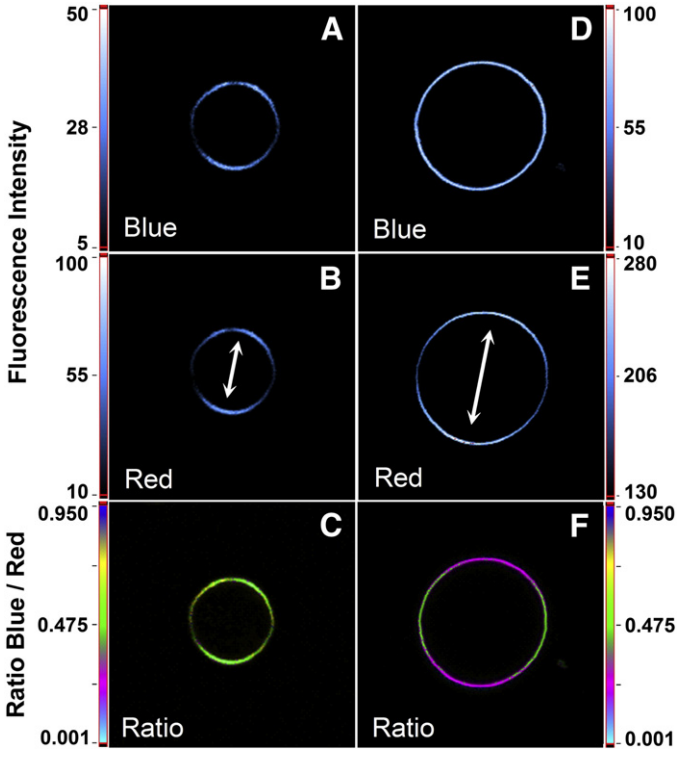


**Fig. 10.** Fluorescence microscopy imaging of MFL-labeled poly-L-lysine (A, B, C) and melittin (D, E, F) bound to DOPC/DOPS (80/20 mol%) GUVs. Intensity images at the blue (<585 nm, A and D) and red (>585 nm, B and E) channels. In the ratiometric images (C and F), the color of each pixel represents the value of the intensity ratio $I_{blue}/I_{red}$, while the pixel intensity corresponds to the total intensity at both channels. Two-photon excitation wavelength was at 830 nm. Arrows indicate the orientation of the light polarization. Sizes of the images were 70 μm × 70 μm. Concentration of poly-L-lysine and melittin was 0.05 and 0.1 μM, respectively.

## 4. Conclusion

The dual-fluorescence label MFL being attached at the N-terminus of peptides allows monitoring interactions of peptides with lipid bilayers, through a nearly two orders of magnitude increase in its emission intensity and appearance of two bands in its fluorescence spectrum. The high environmental sensitivity of the label allows separating the spectrum into individual components and determining the amounts of the non-hydrated and hydrated populations of the label. Then, the intensity ratio of the two emission bands of the non-hydrated species enables evaluation of the dielectric constant of the label environment and thus, estimation of its position in the lipid bilayer. We found that the N-terminus of melittin and magainin 2 is immersed into the bilayer, while that of poly-L-lysine is localized at the membrane surface. These conclusions are fully in line with parallax quenching measurements. Fluorescence microscopy measurements in giant vesicles further revealed differences in the orientation of the label bound to these two peptides. The proposed methodology for monitoring peptide–membrane interactions can in principle be extended to other peptides and environment-sensitive labels.

## Acknowledgments

This work and VYP were supported by ANR (ANR-07-BLAN-0287, FLU-AA-NT), CNRS, Université de Strasbourg, and the ARCUS program between France, Ukraine and Russia. VGP was supported by Université de Strasbourg for short stays in YM's laboratory. We thank H. de Rocquigny for his help in peptide synthesis.

## References


[1] J.R. Lakowicz, Principles of Fluorescence Spectroscopy, 3rd ed.Springer-Verlag, New York, 2006.
[2] J. Ren, S. Lew, J. Wang, E. London, Control of the transmembrane orientation and interhelical interactions within membranes by hydrophobic helix length, Biochemistry 38 (1999) 5905–5912.
[3] J. Ren, S. Lew, Z. Wang, E. London, Transmembrane orientation of hydrophobic α-helices is regulated both by the relationship of helix length to bilayer thickness and by the cholesterol concentration, Biochemistry 36 (1997) 10213–10220.
[4] H. Zhao, P.K.J. Kinnunen, Binding of the antimicrobial peptide temporin L to liposomes assessed by Trp fluorescence, J. Biol. Chem. 277 (2002) 25170–25177.
[5] K. Matsuzaki, O. Murase, H. Tokuda, S. Funakoshi, N. Fujii, K. Miyajima, Orientational and aggregational states of magainin 2 in phospholipid bilayers, Biochemistry 33 (1994) 3342–3349.
[6] A.S. Ladokhin, S. Jayasinghe, S.H. White, How to measure and analyze tryptophan fluorescence in membranes properly, and why bother? Anal. Biochem. 285 (2000) 235–245.
[7] G. Weber, F.J. Farris, Synthesis and spectral properties of a hydrophobic fluorescent probe: 6-propionyl-2-(dimethylamino)naphthalene, Biochemistry 18 (1979) 3075–3078.
[8] G. Anderluh, A. Barlic, Z. Podlesek, P. Macek, J. Pungercar, F. Gubensek, M.L. Zecchini, M.D. Serra, G. Menestrina, Cysteine-scanning mutagenesis of an eukaryotic pore-forming toxin from sea anemone. Topology in lipid membranes, Eur. J. Biochem. 263 (1999) 128–136.
[9] M. Zibouche, M. Vincent, F. Illien, J. Gallay, J. Ayala-Sanmartin, The N-terminal domain of annexin 2 serves as a secondary binding site during membrane bridging, J. Biol. Chem. 283 (2008) 22121–22127.
[10] A. Holt, R.B.M. Koehorst, T. Rutters-Meijneke, M.H. Gelb, D.T.S. Rijkers, M.A. Hemminga, J.A. Killian, Tilt and rotation angles of a transmembrane model peptide as studied by fluorescence spectroscopy, Biophys. J. 97 (2009) 2258–2266.
[11] A.S. Klymchenko, A.P. Demchenko, Multiparametric probing of intermolecular interactions with fluorescent dye exhibiting excited state intramolecular proton transfer, Phys. Chem. Chem. Phys. 5 (2003) 461–468.
[12] P.-T. Chou, M.L. Martinez, H. Clements, Reversal of excitation behavior of proton-transfer vs. charge-transfer by dielectric perturbation of electronic manifolds, J. Phys. Chem. 97 (1993) 2618–2622.
[13] A.P. Demchenko, Y. Mely, G. Duportail, A.S. Klymchenko, Monitoring biophysical properties of lipid membranes by environment-sensitive fluorescent probes, Biophys. J. 96 (2009) 3461–3470.
[14] A.S. Klymchenko, Y. Mely, A.P. Demchenko, G. Duportail, Simultaneous probing of hydration and polarity of lipid bilayers with 3-hydroxyflavone fluorescent dyes, Biochim. Biophys. Acta 1665 (2004) 6–19.
[15] A.S. Klymchenko, G. Duportail, A.P. Demchenko, Y. Mely, Bimodal distribution and fluorescence response of environment-sensitive probes in lipid bilayers, Biophys. J. 86 (2004) 2929–2941.
[16] V.V. Shynkar, A.S. Klymchenko, C. Kunzelmann, G. Duportail, C.D. Muller, A.P. Demchenko, J.M. Freyssinet, Y. Mely, Fluorescent biomembrane probe for ratiometric detection of apoptosis, J. Am. Chem. Soc. 129 (2007) 2187–2193.
[17] V.V. Shynkar, A.S. Klymchenko, G. Duportail, A.P. Demchenko, Y. Mely, Two-color fluorescent probes for imaging the dipole potential of cell plasma membranes, Biochim. Biophys. Acta 1712 (2005) 128–136.
[18] C.E. Dempsey, The actions of melittin on membranes, Biochim. Biophys. Acta Rev. Biomembr. 1031 (1990) 143–161.
[19] K. Matsuzaki, S. Yoneyama, K. Miyajima, Pore formation and translocation of melittin, Biophys. J. 73 (1997) 831–838.
[20] S.J. Ludtke, K. He, W.T. Heller, T.A. Harroun, L. Yang, H.W. Huang, Membrane pores induced by magainin, Biochemistry 35 (1996) 13723–13728.
[21] S. Frey, L.K. Tamm, Orientation of melittin in phospholipid bilayers. A polarized attenuated total reflection infrared study, Biophys. J. 60 (1991) 922–930.
[22] D. Sengupta, L. Meinhold, D. Langosch, G.M. Ullmann, J.C. Smith, Understanding the energetics of helical peptide orientation in membranes, Proteins 58 (2005) 913–922.
[23] S. Toraya, K. Nishimura, A. Naito, Dynamic structure of vesicle-bound melittin in a variety of lipid chain lengths by solid-state NMR, Biophys. J. 87 (2004) 3323–3335.
[24] H. Raghuraman, A. Chattopadhyay, Orientation and dynamics of melittin in membranes of varying composition utilizing NBD fluorescence, Biophys. J. 92 (2007) 1271–1283.
[25] B. Bechinger, Structure and functions of channel-forming peptides: Magainins, cecropins, melittin and alamethicin, J. Membr. Biol. 156 (1997) 197–211.
[26] H. Raghuraman, A. Chattopadhyay, Melittin: a membrane-active peptide with diverse functions, Biosci. Rep. 27 (2007) 189–223.
[27] W. Zauner, M. Ogris, E. Wagner, Polylysine-based transfection systems utilizing receptor-mediated delivery, Adv. Drug Deliv. Rev. 30 (1998) 97–113.
[28] W. Hartmann, H.J. Galla, Binding of polylysine to charged bilayer membranes. Molecular organization of a lipid peptide complex, Biochim. Biophys. Acta 509 (1978) 474–490.
[29] M.J. Hope, M.B. Bally, G. Webb, P.R. Cullis, Production of large unilamellar vesicles by a rapid extrusion procedure. Characterization of size distribution, trapped volume and ability to maintain a membrane potential, Biochim. Biophys. Acta Biomembr. 812 (1985) 55–65.
[30] K. Kachel, E. Asuncion-Punzalan, E. London, The location of fluorescence probes with charged groups in model membranes, Biochim. Biophys. Acta 1374 (1998) 63–76.
[31] M.I. Angelova, D.S. Dimitrov, Liposome electroformation, Faraday Discuss. Chem. Soc. 81 (1986) 303–311.
[32] M. Fidorra, L. Duelund, C. Leidy, A.C. Simonsen, L.A. Bagatolli, Absence of fluid-ordered/fluid-disordered phase coexistence in ceramide/POPC mixtures containing cholesterol, Biophys. J. 90 (2006) 4437–4451.
[33] A.S. Klymchenko, S. Oncul, P. Didier, E. Schaub, L. Bagatolli, G. Duportail, Y. Mely, Visualization of lipid domains in giant unilamellar vesicles using an environment-sensitive membrane probe based on 3-hydroxyflavone, Biochim. Biophys. Acta 1788 (2009) 495–499.
[34] F.S. Abrams, E. London, Extension of the parallax analysis of membrane penetration depth to the polar region of model membranes: use of fluorescence quenching by a spin-label attached to the phospholipid polar headgroup, Biochemistry 32 (1993) 10826–10831.
[35] A. Chattopadhyay, E. London, Parallax method for direct measurement of membrane penetration depth utilizing fluorescence quenching by spin-labeled phospholipids, Biochemistry 26 (1987) 39–45.
[36] R.D. Kaiser, E. London, Location of diphenylhexatriene (DPH) and its derivatives within membranes: comparison of different fluorescence quenching analyses of membrane depth, Biochemistry 37 (1998) 8180–8190.
[37] D.P. Tieleman, S.J. Marrink, H.J.C. Berendsen, A computer perspective of membranes: molecular dynamics studies of lipid bilayer systems, Biochim. Biophys. Acta Rev. Biomembr. 1331 (1997) 235–270.
[38] B.A. Lewis, D.M. Engelman, Lipid bilayer thickness varies linearly with acyl chain length in fluid phosphatidylcholine vesicles, J. Mol. Biol. 166 (1983) 211–217.
[39] H. Beltz, E. Piemont, E. Schaub, D. Ficheux, B. Roques, J.L. Darlix, Y. Mely, Role of the structure of the top half of HIV-1 cTAR DNA on the nucleic acid destabilizing activity of the nucleocapsid protein NCp7, J. Mol. Biol. 338 (2004) 711–723.
[40] J. Azoulay, J.P. Clamme, J.L. Darlix, B.P. Roques, Y. Mely, Destabilization of the HIV-1 complementary sequence of TAR by the nucleocapsid protein through activation of conformational fluctuations, J. Mol. Biol. 326 (2003) 691–700.
[41] J.P. Clamme, J. Azoulay, Y. Mely, Monitoring of the formation and dissociation of polyethylenimine/DNA complexes by two photon fluorescence correlation spectroscopy, Biophys. J. 84 (2003) 1960–1968.
[42] A.S. Klymchenko, V.G. Pivovarenko, T. Ozturk, A.P. Demchenko, Modulation of the solvent-dependent dual emission in 3-hydroxychromones by substituents, New J. Chem. 27 (2003) 1336–1343.
[43] V.V. Shynkar, A.S. Klymchenko, E. Piemont, A.P. Demchenko, Y. Mely, Dynamics of intermolecular hydrogen bonds in the excited states of 4′-dialkylamino-3-hydroxyflavones. On the pathway to an ideal fluorescent hydrogen bonding sensor, J. Phys. Chem. A 108 (2004) 8151–8159.
[44] A.S. Klymchenko, V.G. Pivovarenko, A.P. Demchenko, Elimination of the hydrogen bonding effect on the solvatochromism of 3-hydroxyflavones, J. Phys. Chem. A 107 (2003) 4211–4216.
[45] D. Volodkin, V. Ball, P. Schaaf, J.C. Voegel, H. Mohwald, Complexation of phosphocholine liposomes with polylysine. Stabilization by surface coverage versus aggregation, Biochim. Biophys. Acta Biomembr. 1768 (2007) 280–290.
[46] O.H. Griffith, P.J. Dehlinger, S.P. Van, Shape of the hydrophobic barrier of phospholipid bilayers (evidence for water penetration in biological membranes), J. Membr. Biol. 15 (1974) 159–192.
[47] A.S. Klymchenko, G. Duportail, T. Ozturk, V.G. Pivovarenko, Y. Mely, A.P. Demchenko, Novel two-band ratiometric fluorescence probes with different location and orientation in phospholipid membranes, Chem. Biol. 9 (2002) 1199–1208.
[48] L.A. Bagatolli, To see or not to see: lateral organization of biological membranes and fluorescence microscopy, Biochim. Biophys. Acta 1758 (2006) 1541–1556.
[49] S. Afonin, R.W. Glaser, M. Berditchevskaia, P. Wadhwani, K.H. Guhrs, U. Mollmann, A. Perner, A.S. Ulrich, 4-Fluorophenylglycine as a label for 19F NMR structure analysis of membrane-associated peptides, ChemBioChem 4 (2003) 1151–1163.
[50] P.K. Mikhailiuk, S. Afonin, A.N. Chernega, E.B. Rusanov, M.O. Platonov, G.G. Dubinina, M. Berditsch, A.S. Ulrich, I.V. Komarov, Conformationally rigid trifluoromethyl-substituted alfa-amino acid designed for peptide structure analysis by solid-state 19F NMR spectroscopy, Angew. Chem. Int. Ed. 45 (2006) 5659–5661.
[51] G.E. Fanucci, D.S. Cafiso, Recent advances and applications of site-directed spin labeling, Curr. Opin. Struct. Biol. 16 (2006) 644–653.
[52] H. Nymeyer, H.X. Zhou, A method to determine dielectric constants in nonhomogeneous systems: application to biological membranes, Biophys. J. 94 (2008) 1185–1193.
[53] I. Konopasek, P. Kvasnicka, E. Amler, A. Kotyk, G. Curatola, The transmembrane gradient of the dielectric constant influences the DPH lifetime distribution, FEBS Lett. 374 (1995) 338–340.